JOURNAL OF CATALYSIS 61, 316–325 (1980)

The Catalytic Oxidation of Propylene

VI. Mechanistic Studies Utilizing Isotopic Tracers

L. DAVID KRENZKE AND GEORGE W. KEULKS

Laboratory for Surface Studies, Department of Chemistry, University of Wisconsin–Milwaukee, Milwaukee, Wisconsin 53201

Received October 11, 1978; revised July 30, 1979

The mechanism of propylene oxidation has been investigated over well-characterized selective oxidation catalysts: $Bi_2Mo_3O_{12}$, Bi_2MoO_6, and $Bi_3FeMo_2O_{12}$. Oxygen-18 and deuterated propylene were used as tracers under steady-state reaction conditions over the temperature range 350 to 450°C. These data indicate that acrolein is formed exclusively via the redox mechanism over the molybdate catalysts and that numerous sublayers of lattice oxygen are involved. Carbon dioxide is formed by the consecutive oxidation of acrolein over $Bi_2Mo_3O_{12}$ and Bi_2MoO_6 and by the consecutive and parallel pathways over $Bi_3FeMo_2O_{12}$. The rate-limiting step of acrolein formation is the abstraction of an allylic hydrogen from propylene.

INTRODUCTION

Investigations into the mechanism of propylene oxidation have been carried out in many industrial and academic laboratories during the past 15 years. The progress of this research has been extensively reviewed (*1–6*) and it is generally accepted that the first and usually rate-determining step is the dissociative chemisorption of propylene to form a symmetrical π-allylic intermediate. The subsequent reactions of this intermediate which lead to acrolein are, however, less clearly understood. Two reaction schemes have been proposed. One involves a second hydrogen abstraction from a terminal carbon atom followed by the incorporation of a lattice oxide ion. The other involves the direct interaction with a molecular oxygen species to form a peroxide or hydroperoxide. The peroxide then decomposes to yield acrolein and water.

The pathway involving lattice oxygen is commonly referred to as the redox mechanism because the catalyst itself acts as the oxidizing agent. Gas-phase oxygen then serves only to reoxidize the reduced catalyst. There is a considerable amount of data which support the redox concept. Peacock *et al.* (*7*) have shown that a bismuth molybdate catalyst can oxidize propylene in the absence of gas-phase oxygen and that the oxygen appearing in the products can be quantitatively replaced in the lattice. The amount of oxygen removed during reduction corresponds to the participation of many sublayers of oxide ions. Reports involving other oxide systems such as iron antimonate (*8*), Bi–W–O, Sn–Sb–O, and Sn–P–O (*9*) have also concluded that these catalysts have the capacity to act as a source of active oxygen. Although these data strongly support the redox mechanism, the most compelling evidence for the participation of lattice oxygen comes from studies of propylene oxidation in the presence of isotopic oxygen.

Keulks (*10*) reported that during the oxidation of propylene over bismuth molybdate at 480°C in the presence of gas-phase oxygen-18, only 2 to 2.5% of the oxygen atoms in the acrolein and carbon dioxide produced were isotopically labeled. This lack of extensive incorporation of oxygen-18 into the reaction products implies the participation of lattice oxide ions in both the selective and nonselective oxidation reactions. Wragg *et al.* (*11*) studied the

0021-9517/80/020316-10$02.00/0

roles of gas-phase oxygen and oxide ions in the oxidation of propylene at 475°C by enriching the gaseous oxygen or the oxide ions of the bismuth molybdate lattice with oxygen-18. Their results indicated that the oxygen incorporated into acrolein was derived from the lattice and not the gas phase. In a more recent study Keulks and Krenzke (*12*) oxidized propylene over α- and γ-phase bismuth molybdates in the presence of gaseous oxygen-18. The experiments were carried out under steady-state reaction conditions and in a manner which allowed the data to be treated quantitatively. The results showed that 16% of the lattice oxygen in the α-phase and 100% of the lattice oxygen in the γ-phase were involved in the formation of both acrolein and carbon dioxide at 430°C.

There is little doubt that lattice oxygen plays an important role in the oxidation of propylene over oxide catalysts at high temperature (425°C). There is, however, a substantial amount of data which indicate that adsorbed oxygen and therefore the peroxide pathway may also be important with some catalysts or under certain reaction conditions. Sancier *et al.* (*13*) reported the results of their oxygen-18 experiments over a silica-supported bismuth molybdate catalyst and suggested that the oxidation of propylene involved adsorbed oxygen at low temperature (320°C), and primarily lattice oxygen at high temperature (400°C). Cant and Hall (*14, 15*) reported that propylene could be oxidized to acrolein over noble metals (Au, Rh, and Ru) supported on low-area α-alumina or silica. As these catalysts do not contain any usable lattice oxygen, only adsorbed or gas-phase oxygen is available as a reactant. The mechanism was investigated by isotopic labeling techniques and found to involve the interaction of an allylic intermediate with a molecular oxygen species to form a peroxide or hydroperoxide, which subsequently decomposed into acrolein and water. Krylov (*16*) and Kugler and co-workers (*17, 18*) have directly observed the formation and interaction of O_2^- and π-allyl complexes on oxide catalysts at room temperature by EPR and infrared spectroscopy. Keulks and Daniel (*19*) have also reported data which strongly suggest the involvement of a peroxide intermediate in propylene oxidation over bismuth molybdate catalysts. They suggested that a peroxide species formed either on the surface or in the gas phase was responsible for the homogeneous gas phase reaction which they observed in the postcatalytic volume.

As indicated above, there is evidence for both the redox and peroxide pathways of selective propylene oxidation. What cannot be determined, however, from the literature data is the relative importance of each pathway on a particular catalyst. There are also difficulties in making direct comparisons between the various studies because of the use of ill-defined catalysts, widely varying reaction conditions, and different types of reactors. Consequently for this study we have chosen well-characterized selective oxidation catalysts and investigated the reaction mechanism over a wide temperature range by using both deuterated propylene and oxygen-18 as tracers under steady-state reaction conditions.

EXPERIMENTAL

1. Catalyst Preparation

The reagents used for catalyst preparation were Mallinckrodt AR grade ammonium paramolybdate, molybdic acid, and ferric nitrate and Fisher Certified bismuth nitrate.

The α-phase bismuth molybdate, $Bi_2Mo_3O_{12}$, was prepared according to the method of Keulks *et al.* (*20*) by coprecipitation from an acidic solution (pH = 1.5) of ammonium paramolybdate and bismuth nitrate. After 20 h of aging, the precipitate was filtered, dried, and then calcined in air for 5 h at 200°C and again for 15 h at 450°C.

The γ-phase bismuth molybdate, Bi_2MoO_6, was prepared according to the method of Batist *et al.* (*21*) by a slurry

reaction between bismuth nitrate and molybdic acid. The resultant precipitate was filtered, dried, and then calcined in air for 2 h at 500°C.

The bismuth iron molybdate catalyst, $Bi_3FeMo_2O_{12}$, was prepared according to Notermann (*22*). Bismuth hydroxide and ferric hydroxide were precipitated from a basic solution of bismuth nitrate and ferric nitrate. After the addition of molybdic acid, the solution, with a final volume of 500 ml and a pH = 6, was refluxed and stirred at 60°C for 20 h and then evaporated at 60°C for 5–7 h (until dry). The resultant mass was dried at 110°C for 2 h and at 250°C for 4 h, ground, and calcined in air at 520°C for 6 h.

2. *Apparatus*

All the experiments were carried out in a single-pass, integral flow reactor at atmospheric pressure. The reactor consisted of 8-mm Pyrex tubing as a preheat volume and catalyst chamber. To minimize the possibility of a homogeneous reaction in the post-catalytic zone (*19*), a section of 1-mm capillary tubing was used below the catalyst bed. The reactor was heated in a tubular furnace, controlled by a Thermoelectric R-100 temperature controller. The temperature of the reaction was monitored by a dual-junction, 1/16-in. sheathed type K thermocouple inserted directly into the catalyst bed. One thermocouple was connected to the temperature controller and the other to a calibrated Simpson pyrometer.

The feed gases, oxygen (Airco, 99.6%), propylene (Mathesen, C. P. grade), and helium diluent (Airco, 99.99%), were used without further purification. The individual gas flows were controlled by Tylan mass flow controllers, Model FC-260. The isotopic tracers, oxygen-18 (90 atom% ^{18}O) from BOC Limited Prochem, London, and 2,3,3,3,-d_4-propylene from Merck, Sharp and Dohme Canada Limited, Montreal, were added to the feed stream by a syringe pump equipped with a 10-cm^3 Hamilton Gastight syringe.

The feed gas composition and product distribution were analyzed by an in-line gas chromatograph (Porapak R column, 0.25 in. × 6 ft at 140°C) interfaced with a Spectra-Physics Autolab System I computing integrator. The isotopic distribution in the reaction products during the tracer experiments was obtained with a Bendix time of flight mass spectrometer, Model MA-1. The output of the mass spectrometer was digitized by a Columbia Scientific Instruments CSI-260 digital readout system which calculated peak maxima and mass numbers. The spectrometer was coupled to the gc reactor system through a Granville–Phillips variable leak valve.

3. *Procedure*

The feed gas composition for the tracer experiments was 0.1 atm propylene, 0.1 atm oxygen, and 0.8 atm helium at a total flow rate of 18 cm^3/min. These conditions were essentially fixed by the cost and availability of the labeled compounds. Because the flow rate was fixed, the size of the catalyst charge was varied with the reaction temperature in order to maintain reasonable conversion levels (10–20%) for these types of experiments.

Before the tracer experiment was begun, the catalyst was lined-out for several hours under the same conditions as would be used in the tracer experiment. During this time, several gc analyses were run to verify that steady-state conditions had been reached and to determine the product distribution. To start the addition of the labeled compound to the feed stream, the syringe pump containing 5–10 cm^3 of labeled compound ($^{18}O_2$ or $C_3D_4H_2$) at atmospheric pressure was activated and the flow of the nonlabeled compound ($^{16}O_2$ or C_3H_6) was diverted from the reactor inlet to a vent via a three-way value. The flow rates of the labeled and nonlabeled gases (1.8 cm^3/min) were matched so that the partial pressures of the reactants remained constant. This procedure allowed a rapid changeover from the nonlabeled gas to the labeled gas while

maintaining the previously established steady-state conditions.

During the oxygen-18 experiments, the entire reactor effluent was diverted to the mass spectrometer sampling system and the concentrations of oxygen-18 in O_2, CO_2, and C_3H_4O were monitored as a function of time. The mass range of 25 to 65 was scanned either every 13 or every 30 s, depending on observed rate of oxygen-18 incorporation, and 10 to 13 scans were run during each 3- to 6- min addition experiment. The amplitudes of the important mass numbers (32, 34, 36, 44, 46, 48, 56, and 58) were corrected by previously determined background levels.

During the deuterated propylene experiments the reactor effluent was directed into the in-line gc. Near the end of the addition period a single gc analysis was made to determine the rates of formation of carbon dioxide and acrolein. The gc was interfaced with the mass spectrometer for these experiments and as the propylene and acrolein peaks were eluted from the T.C. detector, they were mass analyzed. The percentage of $C_3D_4H_2$ in the propylene peak at the time of analysis along with the gc data before and during the addition experiment allowed the rate constants for carbon dioxide and acrolein formation from C_3H_6 and $CD_3—CD{=}CH_2$ to be calculated. The mass analysis of the acrolein peak yielded the relative concentrations of $CD_2{=}CD—CHO$ and $CH_2{=}CD—CDO$.

RESULTS

1. Oxygen-18 Data

The purpose of using oxygen-18 as a tracer in the investigation of propylene oxidation is to determine whether adsorbed or lattice oxygen is the active species involved in CO_2 and C_3H_4O formation. This determination requires that the experiment be quantitative and capable of distinguishing between the participation of a monolayer or less of adsorbed oxygen and an extensive amount of lattice oxygen. This quantity of reactive oxygen with which the incoming gas-phase oxygen-18 equilibrates can be related to the observed rate of oxygen-18 incorporation into the reaction products and the rate of oxygen flow through the catalyst by assuming that the reactive oxygen reservoir acts as an exponential dilution volume. A modification of the equation described by Ritter and Adams (*25*) in their analysis of the operation of an exponential dilution flask used for calibrating gc detectors is

$$\frac{\%\ ^{18}O \text{ in product}}{\%\ ^{18}O \text{ in } O_2} = 1 - \exp(-Ft/V),$$

where

$\%\ ^{18}O$ in product/$\%\ ^{18}O$ in O_2 is determined by the mass analysis of the reactor effluent at time t;

F = the total flow rate of oxygen through the catalyst, which equals the rate of oxygen flow out of the catalyst as oxygenated products (H_2O, CO_2, and C_3H_4O), in μg-atoms/min;

t = the time into the oxygen-18 addition experiment in min; and

V = the amount of catalyst oxygen participating in the formation of a given product, in μg- atoms.

A plot of

$$-\ln\left(1 - \frac{\%\ ^{18}O \text{ in Product}}{\%\ ^{18}O \text{ in } O_2}\right)$$

versus the time, t, into the addition experiment should yield a straight line with a slope of F/V. Figures 1 and 2 are represent-

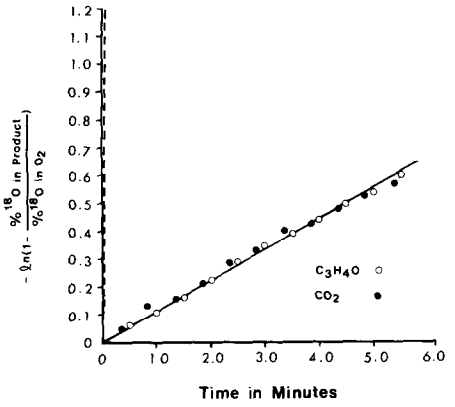

FIG. 1. ^{18}O Incorporation into C_3H_4O and CO_2 over Bi_2MoO_6 at 450°C (○, C_3H_4O; ●, CO_2; and ——, predicted line for a monolayer of oxygen participation).

ative samples of the plots generated from the oxygen-18 data for Bi_2MoO_6 and $Bi_3FeMo_2O_{12}$ at 450, 400, and 350°C. A plot of oxygen-18 data for $Bi_2Mo_3O_{12}$ is not included because it has the same characteristics as the plot for Bi_2MoO_6 shown in Fig. 1.

Utilizing the value of the slope determined from plots like those shown in Fig. 1, a value for the "volume" of catalyst oxygen which participates in the reaction can be obtained. Since the stoichiometry of the catalyst samples used is known, it is possible and convenient to also express the "volume" in terms of the percentage of the total catalyst oxygen which participates in the reaction (columns 6 and 7 in Table 1). We have also found it convenient to convert the "volume" to "number of oxygen layers participating in the reaction" by assuming an oxygen packing density of 1×10^{15} atoms/cm^2 and determining the BET surface area of the catalyst. These values are given in columns 8 and 9 of Table 1. It should be noted that this method requires that the oxygen mobility of the active oxygen be greater than the rate of propylene oxidation. When less than 100% of the catalyst oxygen participates in the reaction, it is not possible to distinguish between the situation where there is a small pool of mobile oxygen and the remainder immobile, and the situation where both surface and lattice oxygen participate. However, kinetic data and other isotopic tracers studies can be coupled with the oxygen-18 experiments to further elucidate the reaction mechanism. The quantity of active catalyst oxygen derived from this treatment of the oxygen-18 data is summarized in Table 1.

It is important to note that the mass analysis of the gas-phase oxygen during the oxygen-18 addition period showed no increase in the signal at mass 34 over the background level. This indicates that the isotopic exchange reaction, $^{32}O_2 + {}^{36}O_2 \rightleftarrows 2{}^{16}O{}^{18}O$, does not occur over these catalysts at the temperatures used in the oxygen-18 addition experiments.

2. *Oxidation of Deuterated Propylene*

The conversion of propylene to acrolein requires the breaking of two carbon–hydrogen bonds and the addition of an oxygen atom. Because it is more difficult to break a C–D than a C–H bond, information about the rate-determining step and the sequence of the hydrogen abstraction and oxygen addition steps can be obtained by comparing the rate constant for acrolein formation

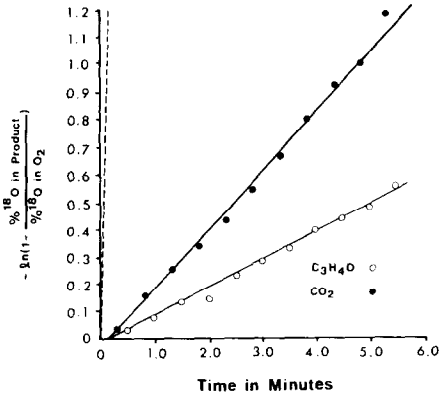

FIG. 2. ^{18}O Incorporation into C_3H_4O and CO_2 over $Bi_3FeMo_2O_{12}$ at 450°C (○, C_3H_4O; ●, CO_2; and ——, predicted line for a monolayer of oxygen participation).

TABLE 1

Summary of Oxygen-18 Data

Catalyst	Reaction temperature (°C)	Weight of catalyst sample (g)	F, Oxygen flow the catalyst (μg-atoms/min)	Percentage selectivity to C_3H_4O	Percentage of catalyst oxygen participating in the formation of		Number of oxygen[a] layers participating in the formation of	
					C_3H_4O	CO_2	C_3H_4O	CO_2
$Bi_2Mo_3O_{12}$	450	0.05	28.7	95	9.4	9.4	47	47
	400	0.10	19.8	88	4.4	4.4	22	22
	350	0.25	13.4	88	2.6	2.6	13	13
Bi_2MoO_6	450	0.05	54.0	91	100	100	282	282
	400	0.075	30.6	92	45	45	126	126
	350	0.15	14.0	91	28	28	79	79
$Bi_3FeMo_2O_{12}$	450	0.05	60.4	86	100	48	72	35
	400	0.10	59.7	86	89	44	64	32
	350	0.20	41.2	82	81	44	58	32

[a] Assuming an oxygen packing density of 1×10^{15} atoms/cm^2 and the following BET surface areas in m^2/g; $Bi_2Mo_3O_{12}$, 1.6; Bi_2MoO_6, 2.1; $Bi_3FeMo_2O_{12}$, 9.4.

from propylene with the rate constant for acrolein formation from deuterated propylene and by examining the distribution of deuterium in acrolein. For this study CD_3—CD=CH_2 was used. Only the deuterium label on the terminal carbon atom is significant for these experiments and choice of this particular compound was based solely on its availability.

The experimentally observed values of the k_H/k_D ratios for the formation of acrolein and carbon dioxide are given in Table 2 and the deuterium distribution of the acrolein is given in Table 3. The theoretical value for the kinetic isotope effect was calculated from molecular data using the method described by Melander (*26*). The deuterated acrolein species observed during the oxidation of $C_3D_4H_2$ were C_3D_3HO and $C_3D_2H_2O$. Therefore, the effect of intermolecular isotopic exchange was negligible.

TABLE 2

Oxidation of 2,3,3,3-d_4-Propylene: k_H/k_D Ratios

	450°C		350°C	
Theoretical primary kinetic isotope effect	1.75		2.14	
Observed isotope effect for the formation of,	C_3H_4O	CO_2	C_3H_4O	CO_2
Over: $Bi_2Mo_3O_{12}$	1.8	1.8	1.7	1.4
Bi_2MoO_6	1.7	1.7	1.5	1.5
$Bi_3FeMo_2O_{12}$	1.7	1.2	2.2	1.2

TABLE 3

Oxidation of 2,3,3,3,-d_4-Propylene: Distribution of Deuterated Acroleins

	450°C		350°C	
	CD_2=CD—CHO (%)	CH_2=CD—CDO (%)	CD_2=CD—CHO (%)	CH_2=CD—CDO (%)
Theoretical distribution obtained for acrolein produced via the redox mechanism	64	36	69	31
Theoretical distribution obtained for acrolein produced via the peroxide mechanism	50	50	50	50
Observed distribution over				
$Bi_2Mo_3O_{12}$	67	33	66	34
Bi_2MoO_6	65	35	64	36
$Bi_3FeMo_2O_{12}$	68	32	67	33

DISCUSSION

1. General Comments on the Isotopic Data

The results of the oxygen-18 and deuterated propylene experiments as they are related to acrolein formation will be discussed in terms of the reaction scheme proposed by Keulks and Daniel (*19*).

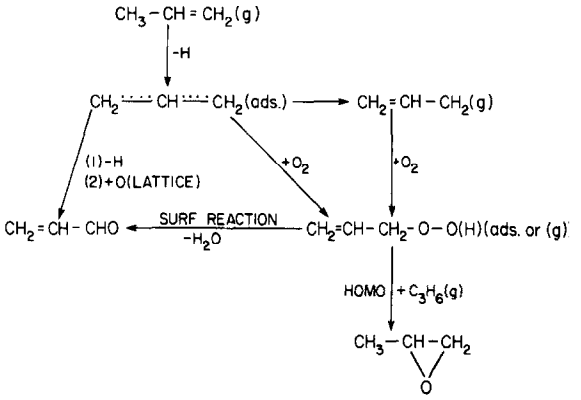

The left-hand portion of the scheme corresponds to the redox mechanism described in the Introduction while the right-hand portion represents the peroxide mechanism.

The initial step of propylene oxidation is the abstraction of a methyl hydrogen to form a symmetrical allylic species. If this is the rate-determining step, then a kinetic isotope effect, k_H/k_D, of 1.8 (2.2) should be observed at 450°C (350°C) for the oxidation of $C_2D_4H_2$. The resulting deuterated allylic species, CD_2–CD–CH_2, can then react further via either the redox pathway or the peroxide pathway. In the peroxide pathway, the deuterated intermediate is at-

tacked by a molecular oxygen species at a terminal carbon atom. Since the deuterium label does not affect the reactivity of the carbon atom itself, each end of the allylic species will react with equal probability. This will lead to a 50–50 distribution of CD_2=CD—CHO and CH_2=CD—CDO. On the other hand, the redox pathway involves an additional hydrogen (deuterium) abstraction from a terminal carbon. In this case, the deuterated carbon atom will react at only 56% (45%) of the rate of the hydrogenated carbon atom at 450°C (350°C). This will lead to a deuterium distribution in acrolein of 64% (69%) CD_2=CD—CHO and 36% (31%) CH_2=CD—CDO at 450°C (350°C).

The redox mechanism and peroxide mechanism can also be differentiated on the basis of the type of oxygen involved. In the redox pathway, lattice oxide ions are incorporated into the product and consequently a large fraction of catalyst oxygen will be involved. The peroxide pathway utilizes adsorbed molecular oxygen and therefore only a monolayer or less of oxygen can participate.

2. *Acrolein and Carbon Dioxide Formation over $Bi_2Mo_3O_{12}$ and Bi_2MoO_6*

The oxygen-18 data in Table 1 clearly indicate that at temperatures between 350 and 450°C multiple layers of lattice oxygen participate in the formation of acrolein and carbon dioxide over α- and γ-bismuth molybdate. Furthermore, there appears to be no distinction between the oxygen incorporated into carbon dioxide and that incorporated into acrolein. This is in agreement with earlier results published by Keulks and Krenzke (*12*) also using the α- and γ-phases of bismuth molybdate.

The oxygen isotope data in Table 1 difinitely show that lattice oxygen, and therefore the redox mechanism, is involved in the oxidation of propylene over bismuth molybdate. However, in only Bi_2MoO_6 at 450°C can it be stated conclusively that *only* the redox mechanism is involved. The other cases, where less than 100% of the catalyst oxygen participates, could be explained by parallel reaction mechanisms, one using lattice oxygen and the other adsorbed oxygen. Consequently, a complete description of the reaction mechanism or mechanisms requires experiments with both oxygen-18 and deuterated propylene.

The deuterium distribution of acrolein formed by the oxidation of 2,3,3,3-d_4-propylene over α- and γ-bismuth molybdate is given in Table 3. A comparison of these data with the theoretical values given for the redox and peroxide mechanisms reveals a close coincidence with the predicted distribution for the redox mechanism. Therefore, on the basis of the oxygen-18 and deuterated propylene experiments, it can be stated that acrolein is formed exclusively via the redox pathway over α- and γ-bismuth molybdate in the temperature range 350 to 450°C.

The data in Table 2 show that a primary kinetic isotope effect is observed for the formation of both carbon dioxide and acrolein. This indicates that the rate-determining step for the formation of both products is the abstraction of a methyl hydrogen from propylene to form the allylic intermediate. Since this allylic intermediate quickly reacts with the catalyst oxygen to form acrolein, the primary pathway of complete combustion appears to be the further oxidation of acrolein. This conclusion was also reached by Keulks *et al.* (*27*) and Soviet scientists (*28–30*) from experimental data involving the oxidation of carbon-14-labeled propylene, acrolein, and acetaldehyde over bismuth molybdate catalysts.

It has already been noted that the oxygen in carbon dioxide is derived from the lattice. Consequently, the complete combustion process must involve a reaction between adsorbed acrolein and lattice oxygen. Haber (*31*) has suggested that the activation of oxygen leads to complete combustion and Kazanskii (*32*) has described a process whereby a regular oxide ion can be converted to the highly reactive

O^- ion via charge transfer. If the O^- ion can indeed be generated from an oxide ion under reaction conditions, then this could easily explain the formation of carbon dioxide from lattice oxygen and acrolein. The feasibility of this pathway is supported by the data of Margolis (*4*). She reported a direct correlation between the rate of complete combustion and the charge transfer energies for a series of molybdate catalysts.

3. *Acrolein and Carbon Dioxide Formation over $Bi_3FeMo_2O_{12}$*

The data given in Table 1 indicate that lattice oxygen participates extensively in the formation of acrolein. In fact, between 81 and 100% of the catalyst oxygen is available for the selective oxidation of propylene within the temperature range 350 to 450°C. These data strongly suggest that acrolein is produced via the redox mechanism. This hypothesis is confirmed by the results of the 2,3,3,3,-d_4-propylene oxidation experiments shown in Table 3. A comparison of the observed deuterium distribution of acrolein formed at 350 and 450°C with the calculated values for the redox mechanism shows an excellent agreement. Therefore, as with the bismuth molybdate catalysts, acrolein formation over $Bi_3FeMo_2O_{12}$ proceeds exclusively by the redox pathway.

Figure 2 seems to indicate that a smaller fraction of lattice oxygen participates in the formation of carbon dioxide than in the formation of acrolein. This, however, may not be the case. At 450°C, 100% of the catalyst oxygen is capable of participating in acrolein formation. Therefore, there can be no separate reservoir of lattice oxygen to account for the different oxygen-18 content of carbon dioxide. The only possible explanation is that the observed rate of oxygen-18 incorporation into carbon dioxide is a composite of the rate of oxygen incorporation from the lattice and of oxygen incorporation from an adsorbed phase. If one assumes that the amount of lattice oxygen involved in carbon dioxide formation is the same as for acrolein formation and that the amount of adsorbed oxygen involved is less than a monolayer, it appears that approximately 50% of the carbon dioxide produced involves a reaction with lattice oxygen and 50% with adsorbed oxygen.

This calculation indicates that two types of oxygen participate in carbon dioxide formation, but it does not give any information as to whether carbon dioxide is produced directly from propylene or by the further oxidation of acrolein. This information can be obtained from the kinetic isotope data given in Table 2. A full primary isotope effect is observed for acrolein formation at both 350 and 450°C. This indicates, as with the bismuth molybdates, that the formation of the allylic intermediate is the rate-determining step. Carbon dioxide formation, however, yields only a partial kinetic isotope effect at both temperatures. This can be explained as the sum of two processes: (1) the consecutive oxidation of acrolein for which a full isotope effect would be expected, and (2) the parallel pathway which would involve an interaction between adsorbed oxygen and the double bond of propylene. Since the C–H or C–D bonds are not immediately involved in the latter process, no isotope effect would be expected. Consequently, it appears that carbon dioxide is produced by both consecutive and parallel pathways over $Bi_3FeMo_2O_{12}$.

CONCLUSIONS

The selective oxidation of propylene to acrolein can occur by either the redox or peroxide mechanism. However only the redox mechanism appears to be operative for $Bi_2Mo_3O_{12}$, Bi_2MoO_6, and $Bi_3FeMo_2O_{12}$. Carbon dioxide appears to be formed solely by the consecutive oxidation of acrolein over the bismuth molybdates and involves only lattice oxygen. With $Bi_3FeMo_2O_{12}$, carbon dioxide is produced by both the consecutive and parallel pathways and involves both lattice and adsorbed oxygen. The rate-determinig step in acrolein forma-

tion over $Bi_2Mo_3O_{12}$, Bi_2MoO_6, and $Bi_3FeMo_2O_{12}$ is the formation of an allylic species via the abstraction of a methyl hydrogen from propylene.

REFERENCES

1. Sampson, R. J., and Shooter, D., *Oxid. Combust. Rev.* **1**, 223 (1965).
2. Voge, H. H., and Adams, C. R., *in* "Advances in Catalysis" (D. D. Eley, H. Pines, and P. B. Weisz, Eds.), Vol. 17, p. 151. Academic Press, New York. 1967.
3. Sachtler, W. M. H., *Catal. Rev.* **4**, 27 (1970).
4. Margolis, L. Ya., *Catal. Rev.* **8**, 241 (1973).
5. Hucknall, D. J., "Selective Oxidation of Hydrocarbons." Academic Press, New York, 1974.
6. Keulks, G. W., Krenzke, L. D., and Notermann, T. M., *in* "Advances in Catalysis" (D. D. Eley, H. Pines, and P. B. Weisz, Eds.), Vol. 27, p. 183. Academic Press, New York, 1978.
7. Peacock, J. M., Parker, A. J., Ashmore, P. G., and Hockey, J. A., *J. Catal.* **15**, 398 (1969).
8. Fattore, V., Fuhrman, Z. A., Manara, G., and Notari, B., *J. Catal.* **37**, 223 (1975).
9. Niwa, M., and Murakami, Y., *J. Catal.* **26**, 359 (1972).
10. Keulks, G. W., *J. Catal.* **19**, 232 (1970).
11. Wragg, R. D., Ashmore, P. G., and Hockey, J. A., *J. Catal.* **22**, 49 (1971).
12. Keulks, G. W., and Krenzke, L. D., *in* "Proceedings, 6th International Congress on Catalysis, London, 1976" (G. C. Bonds, P. B. Wells, and F. C. Tompkins, Eds.). Chem. Soc., London, 1977.
13. Sancier, K. M., Wentrcek, P. R., and Wise, H., *J. Catal.* **39**, 141 (1975).
14. Cant, N. W., and Hall, W. K., *J. Phys. Chem.* **75**, 2914 (1971).
15. Cant, N. W., and Hall, W. K., *J. Catal.* **22**, 310 (1971).
16. Krylov, O. V., *Kinet. Katal.* **14**, 24 (1973).
17. Kugler, B. L., and Kokes, R. J., *J. Catal.* **32**, 170 (1974).
18. Kugler, B. L., and Gryder, J. W., *J. Catal.* **44**, 126 (1976).
19. Keulks, G. W., and Daniel, C., *J. Catal.* **24**, 529 (1971).
20. Keulks, G. W., Hall, J. L., Daniel, C., and Suzuki, K., *J. Catal.* **34**, 79 (1974).
21. Batist, Ph. A., Bouwens, J. F. H., and Schuit, G. C. A., *J. Catal.* **25**, 1 (1972).
22. Notermann, T. M., Ph.D. thesis, University of Wisconsin–Milwaukee, 1976.
23. Grasselli, R. K., and Suresh, D. D., *J. Catal.* **25**, 273 (1972).
24. Grasselli, R. K., and Callahan, J. L., *J. Catal.* **14**, 93 (1969).
25. Ritter, J. J., and Adams, N. K., *Anal. Chem.* **48**, 612 (1976).
26. Melander, L., "Isotope Effects on Reaction Rates," p. 22. Ronald Press, New York, 1960.
27. Keulks, G. W., Rosynek, M. P., and Daniel, C., *Ind. Eng. Chem. Prod. Res. Develop.* **10**, 138 (1971).
28. Gorshkov, A. P., Kolchin, I. K., Gribov, I. M., and Margolis, L. Ya., *Kinet. Katal.* **9**, 1087 (1968).
29. Gorshkov, A. P., Kolchin, I. K., Isgulyants, G. V., Derbentsev, Ya. I., and Margolis, L. Ya., *Dokl. Akad. Nauk SSSR* **186**, 827 (1969).
30. Gagarin, S. G., Kolchin, I. K., and Margolis, L. Ya., *Neftekhimiya* **10**, 59 (1970).
31. Haber, J., Z., *fur Chem.* **13**, 241 (1973).
32. Kazanskii, V. B., *Kinet. Katal.* **14**, 72 (1973).